PERGAMON

International Journal of Heat and Mass Transfer 43 (2000) 1439–1448

International Journal of HEAT and MASS TRANSFER

www.elsevier.com/locate/ijhmt

A nonlinear low-Reynolds number heat transfer model for turbulent separated and reattaching flows

Gwang Hoon Rhee, Hyung Jin Sung*

Department of Mechanical Engineering, Korea Advanced Institute of Science and Technology, 373-1 Kusong-dong, Yusong-ku, Taejon 305-701, South Korea

Received 20 November 1998; received in revised form 18 June 1999

Abstract

A nonlinear low-Reynolds number heat transfer model is developed to predict turbulent flow and heat transfer in separated and reattaching flows. The k–ε–f_μ model of Park and Sung (T.S. Park, H.J. Sung, A new low-Reynolds-number model for predictions involving multiple surface, Fluid Dynamics Research 20 (1997) 97–113) is extended to a nonlinear formulation, based on the nonlinear model of Gatski and Speziale (G.B. Gatski, C.G. Speziale, On explicit algebraic stress models for complex turbulent flows, J. Fluid Mech. 254 (1993) 59–78). The limiting near-wall behavior is resolved by solving the f_μ elliptic relaxation equation. An improved explicit algebraic heat transfer model is proposed, which is achieved by applying a matrix inversion. The scalar heat fluxes are not aligned with the mean temperature gradients in separated and reattaching flows; a full diffusivity tensor model is required. The near-wall asymptotic behavior is incorporated into the f_λ function in conjunction with the f_μ elliptic relaxation equation. Predictions of the present model are cross-checked with existing measurements and DNS data. The model performance is shown to be satisfactory.

Keywords: Nonlinear turbulence model; Separated and reattaching flow; Convective heat transfer; Low-Reynolds-number model

1. Introduction

In a multi-prong attack on the problem of turbulent flow and heat transfer processes in separated and reattaching flows, a linear k–ε–f_μ model has been developed by Park and Sung [1]. In their model, the near-wall effect without reference to distance and the nonequilibrium effect were incorporated. The main emphasis was placed on the formulation of the elliptic relaxation f_μ equation, together with the presentation of nonlocal near-wall effects in a general coordinate system. However, the linear k–ε–f_μ model has some deficiencies. The anisotropic characteristics of Reynolds stresses were not properly resolved in the recirculating region. Efforts are now directed to extending the linear model to a nonlinear formulation.

A literature survey reveals that many nonlinear or anisotropic eddy-viscosity models have been studied [2–4]. The nonlinear model of Gatski and Speziale [3] is notable, which satisfies both the realizability and necessary invariance requirements. A modified version of their model is employed in the present study, which was made by eliminating the inconsistent rotation term [3,5]. Based on the nonlinear model of Gatski and Speziale, the near-wall treatment is included in conjunc-

* Corresponding author. Tel.: +82-42-869-3027; fax: +82-42-869-5027.

E-mail address: hjsung@cais.kaist.ac.kr (H.J. Sung).

0017-9310/00/$ - see front matter
PII: S0017-9310(99)00223-9

Nomenclature

c	specific heat
C_f	mean skin friction coefficient
C_μ, C_{ε_1}, C_{ε_2}	model constants
f_μ, f_2	model functions
H	height of backward-facing step
h	heat transfer coefficient ($= q_w/(T_w - T_\infty)$)
k	turbulent kinetic energy
P_t	turbulent Prandtl number ($= \nu_t/\alpha_t$)
P_k	production of turbulent energy ($= -\overline{u_i u_j}\partial U_i/\partial x_j$)
R_t	turbulent Reynolds number ($= k^2/\nu\varepsilon$)
S_{ij}	strain rate tensor ($= 0.5(U_{i,j} + U_{j,i})$)
St	Stanton number ($= h/U\rho c$)
T	mean temperature
X_R	reattachment length

Greek symbols

α_t	thermal eddy diffusivity
δ	boundary layer thickness
ε	dissipation rate of turbulent energy
ρ	density
σ_k, σ_ε	model constants of turbulent diffusion
ω_{ij}	vorticity tensor ($= 0.5(U_{i,j} - U_{j,i})$)

tion with the wall elliptic relaxation f_μ equation. A nonlinear low-Reynolds number k–ε–f_μ model is proposed, which combines the nonlinear model of Gatski and Speziale [3] and the linear k–ε–f_μ model of Park and Sung [1].

It is known that a simple gradient transport model predicts well the scalar heat flux in homogeneous flows. Turbulent heat transfer is oftentimes simulated by employing the turbulent Prandtl number P_t, by which the thermal diffusivity is prescribed by the known eddy viscosity. This assumption satisfies Pope's linear superposition principle of scalars in turbulent flows [6]. However, these are not adequate to predict convective heat transfer in separated and reattaching flows. This is because the scalar heat fluxes are no longer aligned with the mean temperature gradients. Moreover, the magnitude of the flux component down the gradient varies substantially, depending on the direction of the imposed mean temperature gradient [7]. In the present study, a diffusivity tensor model is brought forth to implement the orientation of mean temperature gradient with respect to the mean temperature. Starting from an algebraic heat transfer model, an explicit diffusivity tensor model is obtained by applying a matrix inversion. To secure an accurate prediction near the wall, a thermal damping function f_λ is incorporated in conjunction with the prior f_μ elliptic relaxation function. The present model is tested for the turbulent flow behind a backward-facing step by comparing the predictions with the experimental data of Vogel and Eaton [8].

2. Nonlinear k–ε–f_μ model

A stationary and incompressible turbulent flow is considered, where the Reynolds-averaged Navier–Stokes and continuity equations can be written in the form [1]:

$$U_j\frac{\partial U_i}{\partial x_j} = -\frac{1}{\rho}\frac{\partial P}{\partial x_i} + \nu\nabla^2 U_i - \frac{\partial \tau_{ij}}{\partial x_j}, \tag{1}$$

$$\frac{\partial U_i}{\partial x_i} = 0, \tag{2}$$

where U_i is the mean velocity, P the mean pressure and ν the kinetic viscosity of the fluid, respectively. The Reynolds stress tensor ($\tau_{ij} = \overline{u_i u_j}$) can be represented by the eddy viscosity form [1]:

$$\tau_{ij} = \frac{2}{3}k\delta_{ij} - 2\nu_t S_{ij}, \tag{3}$$

where

$$S_{ij} = \frac{1}{2}\left(\frac{\partial U_i}{\partial x_j} + \frac{\partial U_j}{\partial x_i}\right) \tag{4}$$

is the mean rate of strain tensor. ν_t is the eddy viscosity, which is given by

$$\nu_t = C_\mu f_\mu \frac{k^2}{\varepsilon}, \tag{5}$$

where the coefficient C_μ is a constant ($C_\mu = 0.09$).

A wall damping function f_μ is introduced in Eq. (5) to describe the damping of eddy viscosity near the wall. f_μ must approach 1 far away from the wall so that the standard k–ε model form is recovered. However, in complex separated and reattaching flows, a local equilibrium ($P_k = \varepsilon$) is not guaranteed [1]. In an effort to incorporate these nonequilibrium effect ($P_k \neq \varepsilon$), variations of C_μ are allowed by decomposing f_μ into $f_\mu = f_{\mu_1} f_{\mu_2}$, in which f_{μ_1} signifies the effect of wall proximity in the near-wall region while f_{μ_2} rep-

resents the effect of nonequilibrium away from the wall [1]:

$$f_{\mu_1} = \left(1 + 20\exp\left[-(R_t/120)^2\right]R_t^{-3/4}\right)f_w^2, \tag{6}$$

$$f_{\mu_2} = 7.0\frac{4.5 + 0.3P_k/\varepsilon}{(4.5 + 1.3P_k/\varepsilon)^2}. \tag{7}$$

In the above, R_t is the turbulent Reynolds number $R_t = k^2/\nu\varepsilon$. To avoid the empiricism associated with defining the wall distance, a Helmholtz-type elliptic relaxation equation for f_w was introduced by Park and Sung [1], which is a general ellipticity for f_w without knowledge of the wall distance:

$$L^2\nabla^2 f_w = \frac{R_t^{3/2}}{A^2}(f_w - 1). \tag{8}$$

Here, A is the model constant $A = 0.8$. L is the turbulent length scale $L = k^{3/2}/\varepsilon$. However, as the wall is approached, k goes to zero, while ε remains finite. Hence, this scale tends to zero. In order to handle the singularity close to the wall, the Kolmogorov length scale is adopted as the lower bound [9]:

$$L^2 = 0.2^2\left[\frac{k^3}{\varepsilon^2} + 70^2\left(\frac{\nu^2}{\varepsilon}\right)^{1/2}\right]. \tag{9}$$

The details regarding the model formulation are compiled in Park and Sung [1].

For a more accurate simulation of separated and reattaching flows, it is important to account for the nonlinear behavior of eddy viscosity. The general form of τ_{ij} is expanded as

$$\tau_{ij} = \frac{2}{3}k\delta_{ij} - 2\nu_t S_{ij} + \tau_{ij}^N, \tag{10}$$

where τ_{ij}^N is the nonlinear part of the deviatoric Reynolds stress tensor which is traceless [3]:

$$\begin{aligned}\tau_{ij}^N &= \alpha_1\frac{k^3}{\varepsilon^2}(S_{ik}\omega_{kj} + S_{jk}\omega_{ki}) \\ &+ \alpha_2\frac{k^3}{\varepsilon^2}\left(S_{ik}S_{kj} - \frac{1}{3}S_{kl}S_{kl}\delta_{ij}\right) \\ &+ \alpha_3\frac{k^3}{\varepsilon^2}\left(\omega_{ik}\omega_{kj} - \frac{1}{3}\omega_{kl}\omega_{kl}\delta_{ij}\right).\end{aligned} \tag{11}$$

The mean vorticity tensor ω_{ij} is $\omega_{ij} = 0.5(\partial U_i/\partial x_j - \partial U_j/\partial x_i)$. The coefficients α_1, α_2 and α_3 are constants and δ_{ij} denotes the Kronecker delta. Eq. (11) has the similar form to the expression derived by Rubinstein and Barton [10] and Yoshizawa [11]. Speziale asserted that the last term in Eq. (11) shows physically inconsistent results and unrealizable solutions in rotating flows [5]. This suggests $\alpha_3 = 0$. Based on the nonlinear model of Gatski and Speziale [3], the afore-stated near-wall effect ($k^2/\varepsilon \sim \nu_t$) is included in concert with the wall relaxation elliptic f_μ equation. A nonlinear k–ε–f_μ model is proposed, where the nonlinear model of Gatski and Speziale [3] and the linear k–ε–f_μ model [1] are combined together:

$$\begin{aligned}\tau_{ij}^N &= \alpha_1\frac{k}{\varepsilon}\nu_t(S_{ik}\omega_{kj} + S_{jk}\omega_{ki}) \\ &+ \alpha_2\frac{k}{\varepsilon}\nu_t\left(S_{ik}S_{kj} - \frac{1}{3}S_{kl}S_{kl}\delta_{ij}\right),\end{aligned} \tag{12}$$

where

$$\alpha_1 = -\frac{1}{2}S_p\left(\frac{4}{3} - C_{\alpha_2}\right)g^2, \tag{13}$$

$$\alpha_2 = 2\alpha_1\frac{2 - C_{\alpha_3}}{2 - C_{\alpha_4}}, \tag{14}$$

$$g^{-1} = \frac{1}{2}C_{\alpha_1} + \frac{C_{\varepsilon_2} - 1}{C_{\varepsilon_1}^* - 1} - 1. \tag{15}$$

The model constants C_{α_1}, C_{α_2}, C_{α_3}, C_{α_4} and S_p are taken from the pressure–strain model [12]:

$$\begin{aligned}&C_{\alpha_1} = 6.6,\ C_{\alpha_2} = 0.36,\ C_{\alpha_3} = 1.25,\ C_{\alpha_4} = 0.40, \\ &S_p = 2.22.\end{aligned} \tag{16}$$

The turbulent kinetic energy equation and its dissipation rate equation are:

$$U_j\frac{\partial k}{\partial x_j} = \frac{\partial}{\partial x_j}\left[\left(\nu + \frac{\nu_t}{\sigma_k}\right)\frac{\partial k}{\partial x_j}\right] + P_k - \varepsilon, \tag{17}$$

$$\begin{aligned}U_j\frac{\partial \varepsilon}{\partial x_j} &= \frac{\partial}{\partial x_j}\left[\left(\nu + \frac{\nu_t}{\sigma_\varepsilon}\right)\frac{\partial \varepsilon}{\partial x_j}\right] + C_{\varepsilon_1}^* P_k\frac{\varepsilon}{k} \\ &- C_{\varepsilon_2}f_2\frac{\varepsilon^2}{k} + C_1(1 - f_w)\nu\nu_t\left(\frac{\partial^2 U_i}{\partial x_j\partial x_k}\right)^2,\end{aligned} \tag{18}$$

where the model constants σ_k, σ_ε, C_{ε_1}, C_{ε_2} and C_1 are:

$$\begin{aligned}&\sigma_k = 1.2,\ \sigma_\varepsilon = 1.3,\ C_{\varepsilon_1} = 1.45,\ C_{\varepsilon_2} = 1.8, \\ &C_1 = 0.4.\end{aligned} \tag{19}$$

It is seen that the nonequilibrium effect is also incorporated in $C_{\varepsilon_1}^*$, which has the form $C_{\varepsilon_1}^* = C_{\varepsilon_1} - \frac{\eta(1-\eta/4.44)}{1+0.25\eta^3}$. η is the ratio of the turbulent to mean strain time scale ($\eta = \sqrt{2S_{ij}S_{ij}}k/\varepsilon$). The model function f_2 in Eq. (18) is expressed as $f_2 = 1 - \frac{2}{9}\exp(-0.33R_t^{1/2})$. The wall boundary conditions are: $U = V = k = 0$ and

$\varepsilon = \nu\partial^2 k/\partial n^2$, where n is the wall normal direction. Details can be found in Park and Sung [1].

3. Explicit algebraic heat transfer model

As remarked earlier, simple gradient-transport-type models are inadequate in predicting convective heat transfer in separated and reattaching flows. A tensor diffusivity model is needed to implement the orientation of mean temperature gradient with respect to the mean temperature. To achieve a full diffusivity tensor model resulting from mean temperature gradients aligned with each of the coordinate directions, an algebraic heat flux model is employed [7],

$$P_{i\theta} + \phi_{i\theta} - \varepsilon_{i\theta} = \frac{\overline{u_i\theta}}{2k}(P_k - \varepsilon) + \frac{\overline{u_i\theta}}{2k_\theta}(P_\theta - \varepsilon_\theta), \tag{20}$$

where $P_{i\theta}$, $\phi_{i\theta}$ and $\varepsilon_{i\theta}$ denote the production of $\overline{u_i\theta}$, pressure–temperature-gradient and dissipation of $\overline{u_i\theta}$, respectively. P_θ is the production of temperature variance ($P_\theta = -\overline{u_i\theta}\partial T/\partial x_i$) and ε_θ is the dissipation rate of temperature variance.

It is stressed that the effect of nonequilibrium of the velocity field (P_k/ε) has been fully accounted for in the afore-stated velocity model. Accordingly, the nonequilibrium effect of passive scalar field ($P_\theta/\varepsilon_\theta$) is neglected in the present study to avoid these duplicate considerations. Furthermore, the thermal nonequilibrium can be resolved by solving the full turbulent diffusivity tensor model. The thermal equilibrium condition, i.e., $P_\theta/\varepsilon_\theta = 1$, also satisfies Pope's linear superposition principle of passive scalars in turbulent flow [6]. Eq. (20) can then be simplified to

$$\overline{u_i\theta} = \frac{2k/\varepsilon\left(P_{i\theta} + \phi_{i\theta} - \varepsilon_{i\theta}\right)}{(P_k/\varepsilon - 1)}. \tag{21}$$

If the model of Gibson and Launder for $\phi_{i\theta} - \varepsilon_{i\theta}$ is adopted, i.e., $\phi_{i\theta} - \varepsilon_{i\theta} = -C_{1\theta}\frac{\varepsilon}{k}\overline{u_i\theta} - C_{2\theta}P_{i\theta}$ [13], the resulting equation after arrangement takes the form:

$$\frac{C_{1\theta}}{1 - C_{2\theta}}\frac{\varepsilon}{k}\overline{u_i\theta} = -\overline{u_j\theta}\frac{\partial U_i}{\partial x_j} - \overline{u_iu_j}\frac{\partial T}{\partial x_j}, \tag{22}$$

where $C_{1\theta}$ and $C_{2\theta}$ are model constants, $C_{1\theta} = 3.0$ and $C_{2\theta} = 0.33$ [13].

In matrix form, Eq. (22) can be expressed in a non-dimensional form:

$$\begin{bmatrix} \frac{\partial U^*}{\partial x} + 1 & \frac{\partial U^*}{\partial y} & \frac{\partial U^*}{\partial z} \\ \frac{\partial V^*}{\partial x} & \frac{\partial V^*}{\partial y} + 1 & \frac{\partial V^*}{\partial z} \\ \frac{\partial W^*}{\partial x} & \frac{\partial W^*}{\partial y} & \frac{\partial W^*}{\partial z} + 1 \end{bmatrix} \begin{bmatrix} b^*_{1\theta} \\ b^*_{2\theta} \\ b^*_{3\theta} \end{bmatrix} = -\begin{bmatrix} \tau^*_{11} & \tau^*_{12} & \tau^*_{13} \\ \tau^*_{21} & \tau^*_{22} & \tau^*_{23} \\ \tau^*_{31} & \tau^*_{32} & \tau^*_{33} \end{bmatrix} \begin{bmatrix} \frac{\partial T^*}{\partial x} \\ \frac{\partial T^*}{\partial y} \\ \frac{\partial T^*}{\partial z} \end{bmatrix}, \tag{23}$$

where $b^*_{i\theta}$ is defined as $b^*_{i\theta} \equiv \overline{u_i\theta}/2\sqrt{k}T_{\text{ref}}$ and τ_{ij} is $\tau^*_{ij} \equiv \overline{u_iu_j}/2k$. T_{ref} denotes a reference temperature. The dimensionless rescaled gradient variables are:

$$\frac{\partial T^*}{\partial x_j} \equiv \frac{1 - C_{2\theta}}{C_{1\theta}}\frac{k^{3/2}}{\varepsilon}\frac{1}{T_{\text{ref}}}\frac{\partial T}{\partial x_j}, \tag{24}$$

$$\frac{\partial U^*_i}{\partial x_j} \equiv \frac{1 - C_{2\theta}}{C_{1\theta}}\frac{k}{\varepsilon}\frac{\partial U_i}{\partial x_j}. \tag{25}$$

The above algebraic heat transfer model is implicit in nature since the turbulent heat flux tensor appears on both sides of Eq. (22). When the model is applied to nonequilibrium turbulent flows with localized strain rates that are large, the predictive capabilities would be low [3]. An explicit algebraic model is required, which is achieved by applying a matrix inversion [7]:

$$\begin{bmatrix} b^*_{1\theta} \\ b^*_{2\theta} \\ b^*_{3\theta} \end{bmatrix} = f_\lambda C_D^{-1} \begin{bmatrix} \alpha_{11} & \alpha_{12} & \alpha_{13} \\ \alpha_{21} & \alpha_{22} & \alpha_{23} \\ \alpha_{31} & \alpha_{32} & \alpha_{33} \end{bmatrix} \times \begin{bmatrix} \tau^*_{11} & \tau^*_{12} & \tau^*_{13} \\ \tau^*_{21} & \tau^*_{22} & \tau^*_{23} \\ \tau^*_{31} & \tau^*_{32} & \tau^*_{33} \end{bmatrix} \begin{bmatrix} \frac{\partial T^*}{\partial x} \\ \frac{\partial T^*}{\partial y} \\ \frac{\partial T^*}{\partial z} \end{bmatrix}. \tag{26}$$

However, it is seen that a clear determinant of $[\alpha_{ij}]$ is not attained due to the unknown velocity gradient terms in Eq. (23). An alternative can be estimated by taking a factor of the model function C_D. The gradient transport form has been directly derived from the governing equation for the passive scalar flux, with the assumption that the sum of the modelled terms can be represented by a vector aligned with $b^*_{i\theta}$ [14]. This choice is consistent with those by Rogers et al. [14] and Rhee and Sung [7], after which a modified version is proposed in the present study.

The coefficient C_D was proposed by Rogers et al.

[14], which is a function of R_t. The behavior of C_D for all scalar simulation in homogeneous shear flow was described as

$$C_D = a_1\left(1+\frac{a_2}{R_t Pr}\right)^{a_3}\left(1+\frac{a_4}{R_t^{a_5}}\right)^{a_6}, \tag{27}$$

where Pr denotes the Prandtl number. It is found that the linearity and independence principles set forth by Pope are not violated in the C_D formulation [6]. The model constants a_1–a_6 are determined by fitting the DNS data [15,16]; $a_1 = 4$, $a_2 = 130$, $a_3 = 0.25$, $a_4 = 19$, $a_5 = 5.5/8$ and $a_6 = -2$.

The matrix α_{ij} in Eq. (26) is represented as

$$\alpha_{11} = \left(\frac{\partial V^*}{\partial y}+1\right)\left(\frac{\partial W^*}{\partial z}+1\right) - \frac{\partial V^*}{\partial z}\frac{\partial W^*}{\partial y},$$

$$\alpha_{12} = \frac{\partial U^*}{\partial y}\left(\frac{\partial W^*}{\partial z}+1\right) - \frac{\partial U^*}{\partial z}\frac{\partial W^*}{\partial y},$$

$$\alpha_{13} = \frac{\partial U^*}{\partial y}\frac{\partial V^*}{\partial z} - \frac{\partial U^*}{\partial z}\left(\frac{\partial V^*}{\partial y}+1\right),$$

$$\alpha_{21} = \frac{\partial V^*}{\partial x}\left(\frac{\partial W^*}{\partial z}+1\right) - \frac{\partial V^*}{\partial z}\frac{\partial W^*}{\partial x},$$

$$\alpha_{22} = \left(\frac{\partial U^*}{\partial x}+1\right)\left(\frac{\partial W^*}{\partial z}+1\right) - \frac{\partial U^*}{\partial z}\frac{\partial W^*}{\partial x},$$

$$\alpha_{23} = \left(\frac{\partial U^*}{\partial x}+1\right)\frac{\partial V^*}{\partial z} - \frac{\partial U^*}{\partial z}\frac{\partial V^*}{\partial x},$$

$$\alpha_{31} = \frac{\partial V^*}{\partial x}\frac{\partial W^*}{\partial y} - \left(\frac{\partial V^*}{\partial y}+1\right)\frac{\partial W^*}{\partial x},$$

$$\alpha_{32} = \left(\frac{\partial U^*}{\partial x}+1\right)\frac{\partial W^*}{\partial y} - \frac{\partial U^*}{\partial y}\frac{\partial W^*}{\partial x},$$

$$\alpha_{33} = \left(\frac{\partial U^*}{\partial x}+1\right)\left(\frac{\partial V^*}{\partial y}+1\right) - \frac{\partial U^*}{\partial y}\frac{\partial V^*}{\partial x}. \tag{28}$$

If the continuity equation is applied to the above equation, α_{ij} can then be rearranged in a simple tensor form,

$$\alpha_{ij} = \delta_{ij} - \frac{\partial U_i^*}{\partial x_j} + \frac{1}{2}\varepsilon_{imn}\varepsilon_{jkl}\frac{\partial U_k^*}{\partial x_m}\frac{\partial U_l^*}{\partial x_n}. \tag{29}$$

It is interesting to see that α_{ij} is decomposed into three parts. The first term is diagonal. When only this term exists, a linear relation holds between turbulent heat flux and mean temperature gradient. The off-diagonal components of α_{ij} are formed by the rescaled mean velocity terms, in which the third term vanishes under the two-dimensional flow condition.

The direct substitution of α_{ij} into Eq. (26) yields the equation for $b_{j\theta}^*$:

$$-b_{j\theta}^* = f_\lambda C_D^{-1}\left(\delta_{jp}\tau_{pq}^*\frac{\partial T^*}{\partial x_q} - \frac{\partial U_j^*}{\partial x_p}\tau_{pq}^*\frac{\partial T^*}{\partial x_q} + \frac{1}{2}\varepsilon_{jmn}\varepsilon_{pkl}\frac{\partial U_k^*}{\partial x_m}\frac{\partial U_l^*}{\partial x_n}\tau_{pq}^*\frac{\partial T^*}{\partial x_q}\right). \tag{30}$$

The first term on the right-hand side of Eq. (30) plays a dominant role in predicting the scalar heat flux in homogeneous flows, in which the stress term is aligned with the turbulent heat flux. Accordingly, a simple transport-type model can be formulated with the constant turbulent Prandtl number assumption. However, this model is deficient in predicting convective heat transfer in complex separated and reattaching flows. As mentioned earlier, the scalar heat fluxes are no longer aligned with the mean temperature gradients, i.e., the diffusivity tensor does not have to be diagonal. Moreover, the magnitude of the flux component down the gradient varies substantially, depending on the direction of the imposed mean temperature gradient.

Finally, the formulation of f_λ is inspected. A literature survey indicates that explicit heat transfer models have been in use [14,17–19]. However, these preceding studies have not been extended to near-wall flows with the afore-stated full diffusivity tensor model. In practical engineering applications, the ability to integrate the model to the wall is most essential in that it impacts directly on the evaluation of heat transfer coefficients. The near-wall effect is incorporated in the f_λ function. It is known that the near-wall asymptotic behavior is derived as $-\overline{v\theta} \propto y^3$, $\partial T/\partial y \propto y^0$ and $C_D^{-1} \propto y^{-4.5}$. To satisfy the thermal near-wall function, $f_\lambda \propto y^{2.5}$. Based on the elliptic relaxation equation for f_w in Eq. (8), the final form of f_λ is modeled as

$$f_\lambda = f_w^{2.5}. \tag{31}$$

4. Results and discussion

The proposed model is tested for the case of the backward-facing flow, which is frequently used in benchmarking the performance of turbulence models for separated and reattaching flows. The model predictions are compared with the experimental data of Vogel and Eaton [8]. The numerical procedure and

boundary conditions are well described in the earlier studies of Rhee and Sung [7,20].

As a validation of the present nonlinear k–ε–f_μ model performance, distributions of the wall shear stress coefficient (C_f) are exhibited in Fig. 1. These are closely related to the prediction of turbulent heat transfer near the wall. The predicted C_f distributions are compared with the experimental data of Vogel and Eaton [8]. A nondimensional streamwise coordinate $X^* = (X - X_R)/X_R$ is employed, where X_R represents the reattachment length. The step-height Reynolds number is $Re_H = 28{,}000$. As seen in Fig. 1, the present nonlinear model prediction in the recirculating region ($-1 \le X^* \le 0$) shows a better agreement with the experiment than the linear k–ε–f_μ model prediction. This may be caused by the fact that the localized strain and rotation rates in the recirculation region are very large. These effects are included in the nonlinear model in conjunction with the f_μ elliptic relaxation function. On the contrary, the predictions in the relaxing region ($0 \le X^* \le 2$) by both models are less satisfactory, resulting in large discrepancies between predictions and experimental data. These overpredictions are due to the deficiencies of the eddy viscosity model arising from the Boussinesq approximation, which appears to be a common feature of reattaching flow calculations [21,22]. In the relaxing region, the nonlinear effects by the strain rates are insignificant, and no differences are found between the two curves, i.e., the linear and nonlinear model predictions.

The profiles of eddy viscosity (ν_t) are shown in Fig. 2 for the recirculating region ($X/H = X_R/H - 2.1$) and the relaxing region ($X/H = X_R/H + 1.9$). Comparisons are made with the experimental data of Driver and Seegmillar [23] for $Re_H = 38{,}000$. It is evident that the nonlinear model results follow the experimental data in the recirculating region. The agreement is better in the recirculating region than in the recovery region.

Comparisons are extended to the distributions of

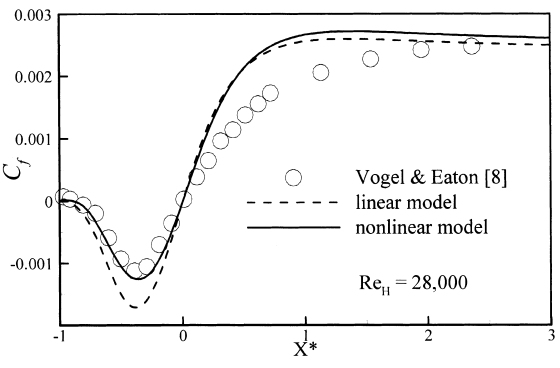

Fig. 1. Comparison of the predicted C_f with experimental data.

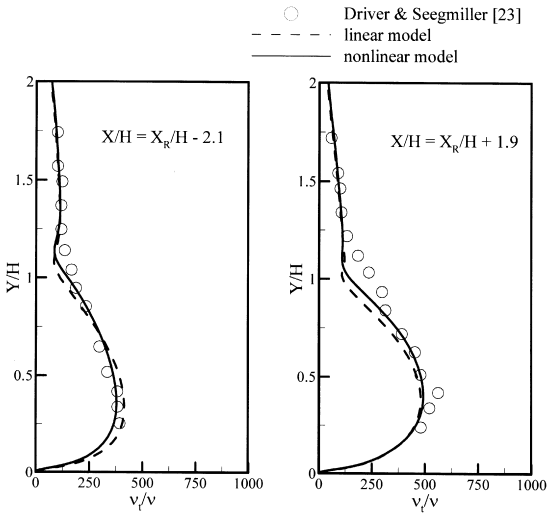

Fig. 2. Comparison of the predicted ν_t with experimental data.

turbulent kinetic energy (k/k_{max}) and corresponding Reynolds shear stress ($\overline{uv}/\overline{uv}_{max}$), as shown in Figs. 3 and 4. The predicted results of turbulent kinetic energy by two models agree reasonably well with the experimental data [24] except in the upper recirculating region. A closer inspection of the profiles in the recirculating region at $X/H = 6$ indicates that the present nonlinear model prediction is in better agreement with the experimental data than the linear model prediction. As for the Reynolds shear stress in Fig. 4, the nonlinear model predictions are more consistent with the experimental data, especially in the recirculating region. These comparisons reinforce the capability of

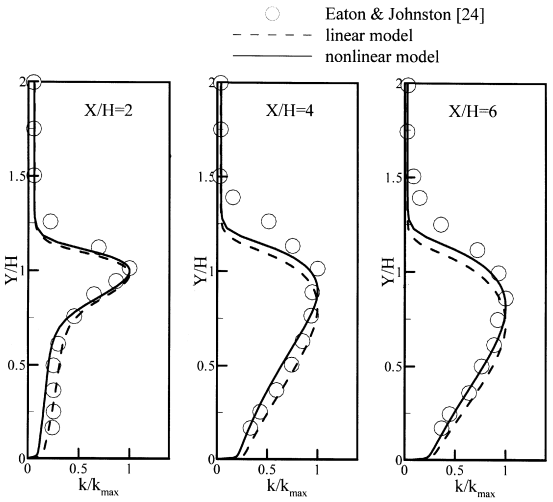

Fig. 3. Comparison of the predicted k with experimental data.

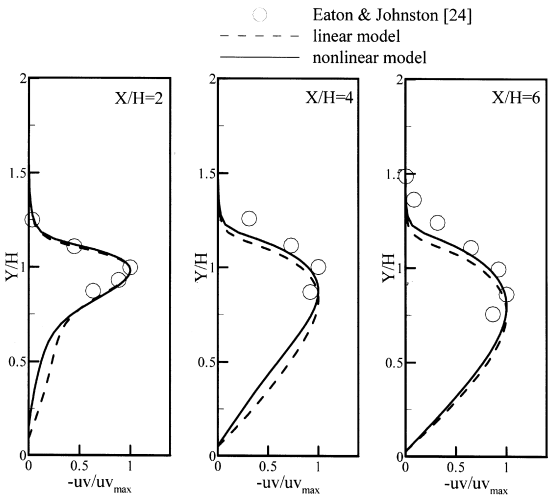

Fig. 4. Comparison of the predicted $-\overline{uv}$ with experimental data.

the present nonlinear model for predicting the recirculating flows over a backward-facing step.

Next, the present heat transfer model performance is investigated for separated and reattaching flows. Before applying the present model to the separated and reattaching flow, the heat transfer characteristics in simple attaching flow is tested by employing the turbulent Prandtl number (Pr_t), in which the thermal diffusivity is prescribed through the known eddy viscosity. An ordinary boundary layer flow, i.e., a fully developed channel flow, is selected. The predicted profiles of temperature T^+ are exhibited in Fig. 5 under two different wall thermal conditions, i.e., uniform wall temperature and uniform wall heat flux. The selected Reynolds numbers are $Re_\tau = 150$ and 180, for which the DNS data are available [15,16]. The predictions by the present model are also displayed for comparisons. As seen in Fig. 5, the constant Prandtl number assumption is reasonable in the fully developed channel flow. The present model shows good agreement with the DNS data, while the constant turbulent Prandtl number model underpredicts slightly in the region of $10 \le y^+ \le 50$. It is noted that the nonlinear model recovers the linear model in a fully developed channel flow, i.e., two models produce the same results.

Further comparison is made in Fig. 6, where the profiles of turbulent heat flux $\overline{v\theta}^+$ in the near wall region are displayed. Both the present model and the constant Prandtl number model provide good agreement with the DNS data. This means that the application of the constant turbulent Prandtl number is acceptable in the attached boundary layer flow. The profiles of the coefficient C_D and the f_λ function are compared with the DNS data (Fig. 7) [16]. It is shown that the near-wall behaviors of ${}^{-1}C_D$ and f_λ are in excellent agreement with the DNS data. These give credence to the model performance close to the wall.

Now, the present heat transfer model is validated in separated and reattaching flows. The Stanton number St profiles are displayed in Fig. 8, where the present diffusivity tensor model is applied to the flow over a backward-facing step. The Stanton number profiles by employing the turbulent Prandtl number $Pr_t = 1.0$, based on the linear and the nonlinear k–ε–f_μ models, are also plotted in Fig. 8. The present model prediction shows an excellent agreement with the experiment. However, it is seen that the predictions with $Pr_t = 1.0$ for both models are in poor agreement with the experiment. These significant overpredictions indicate that the constant Prandtl number assumption is no longer applicable to separated and reattaching flows. However, all of the Stanton number profiles have similar

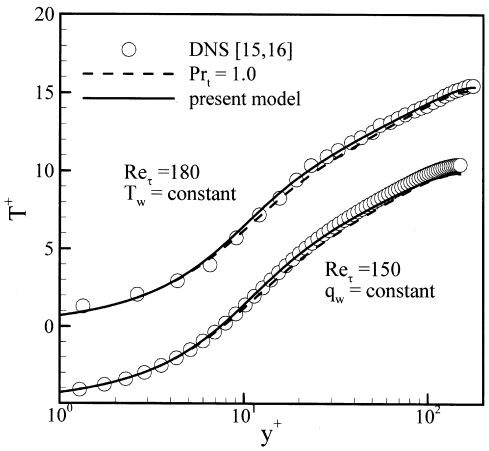

Fig. 5. Comparison of the predicted T with DNS data.

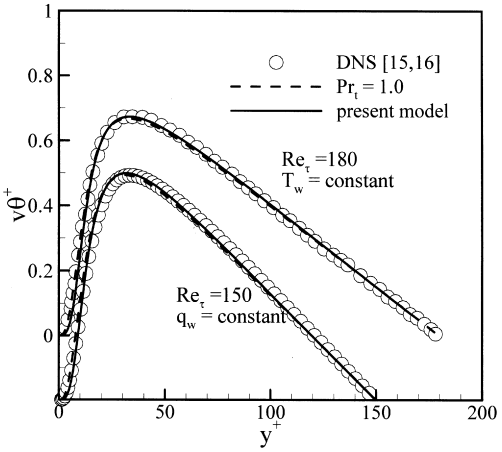

Fig. 6. Comparison of the predicted $-\overline{v\theta}$ with DNS data.

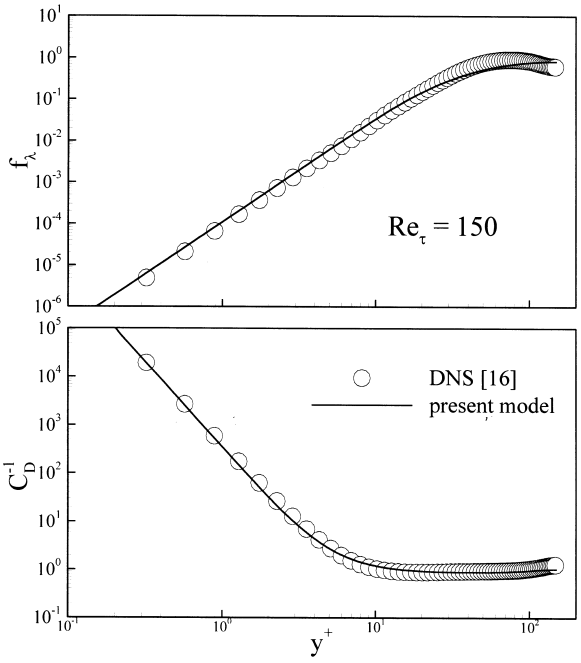

Fig. 7. Comparison of the predicted f_λ and C_D^{-1} with DNS data.

general features, i.e., the peak heat transfer rates occur near the reattachment region ($X^* = 0$) and there is a low heat transfer rate in the recirculation region. The heat transfer coefficient recovers fairly rapidly to the flat-plate behavior downstream of the reattachment [8].

To look into the model performance between the simple transport type model and the present diffusivity tensor model, two model predictions for St are compared in Fig. 9. Here, the simple model is represented by $-b^*_{j\theta} = f_\lambda C_D^{-1} \delta_{jp} \tau^*_{pq} \partial T^* / \partial x_q$, which is composed of the first term in Eq. (30). The discrepancy between the two model predictions is minor, however, the simple

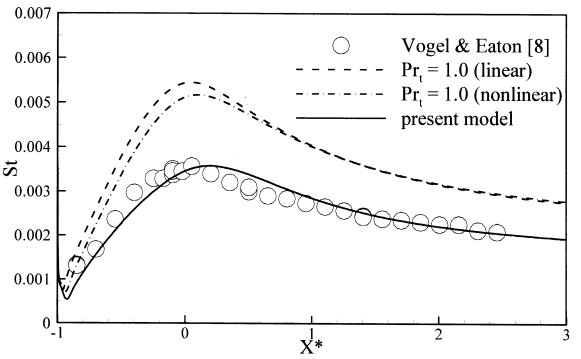

Fig. 8. Comparison of the predicted St with experimental data.

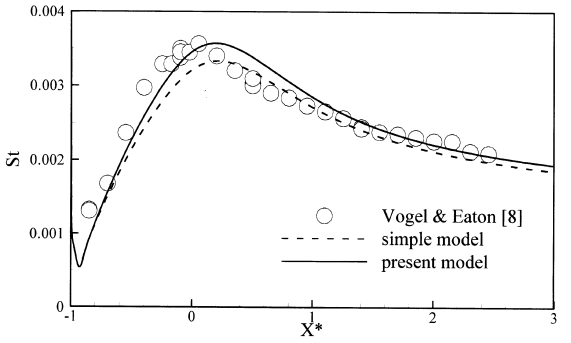

Fig. 9. Model comparisons with experimental data.

model underpredicts slightly in the recirculating region. It is interesting that the maximum Stanton number St_{max} by the present model agrees well with the experiment while the St_{max} profile by the simple model is underpredicted.

Comparisons are made by showing the maximum Stanton number St_{max} in Fig. 10. The maximum Stanton number is plotted by varying Re_H ($13{,}000 \le Re_H \le 42{,}000$). Here, δ/H represents the initial boundary layer thickness normalized by the step height H. It is clearly seen that the present model predictions are in excellent agreement with the experiment. However, the predicted results by $Pr_t = 1.0$ are seen to be slightly overpredicted. The results by the nonlinear k–ε–f_μ model are better than those by the linear model. In general, St_{max} is shown to decrease monotonically as Re_H increases. It is known that St_{max} is a function of Re_H [8].

The Pr_t distribution is useful in understanding the heat transfer characteristics in separated and reattaching flows. The definition of Pr_t in Fig. 11 is $\frac{\overline{uv}}{2S_{12}} / \frac{\overline{v\theta}}{\partial T/\partial y}$. An inspection of the contour plot of Pr_t discloses that the assumption of $Pr_t = constant$ is inadmissible in the

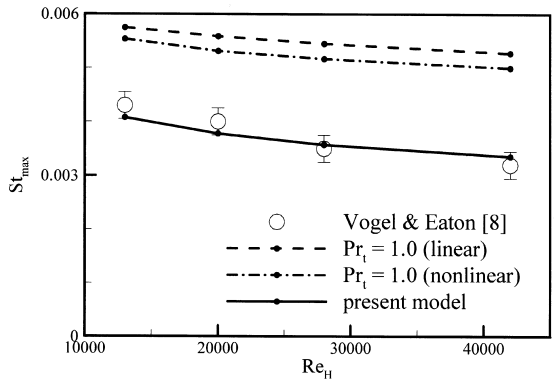

Fig. 10. Comparison of the predicted St_{max} with experimental data.

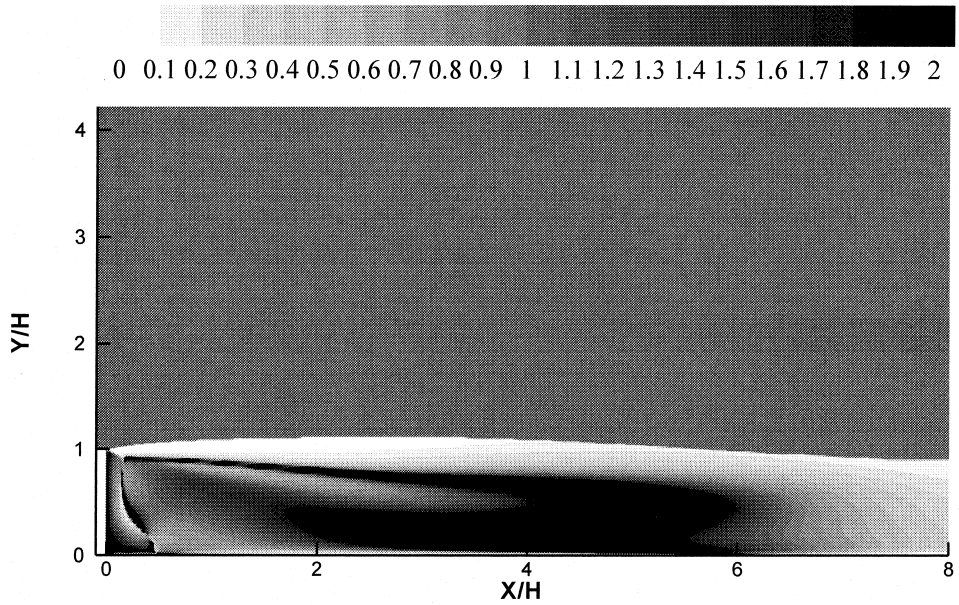

Fig. 11. Distribution of the turbulent Prandtl number (Pr_t).

recirculating region while $Pr_t = constant$ is acceptable outside the recirculating zone. It is found that Pr_t increases considerably in the recirculating region. This may be caused by the enhanced eddy diffusivity.

The profiles of mean temperature are shown in Fig. 12. The step height Reynolds number is $Re_H = 23{,}000$ and the boundary layer thickness is $\delta/H = 1.1$ at the inlet ($X/H = -3.8$). As shown in Fig. 12, the predicted profiles of mean temperature by the present model show better agreement with the experiment than the other two model predictions.

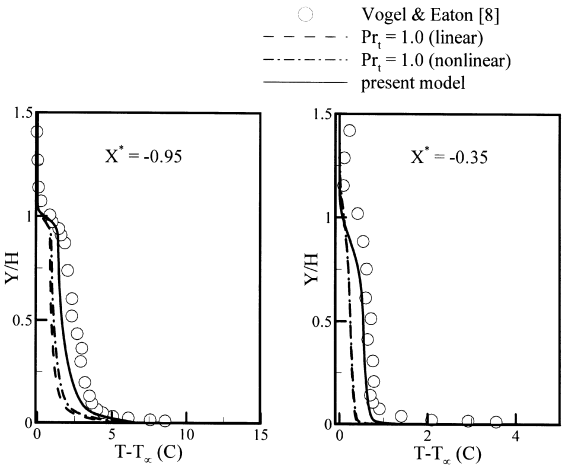

Fig. 12. Comparison of the predicted T with experimental data.

5. Conclusions

A computational study has been made to investigate the predictive capabilities of an explicit diffusivity tensor model to separated and reattaching flows. A new version of nonlinear k–ε–f_μ model was developed. The limiting near-wall behavior close to the wall and the nonequilibrium effect in the recirculating region away from the wall were resolved by solving the elliptic relaxation equation. The nonequilibrium effect in the recirculating region was fully accounted for. The wall limiting behavior of the diffusivity tensor model was also incorporated. The present model was tested against the DNS data of a fully developed channel flow with a uniform wall temperature and with a uniform heat flux. The near-wall behavior of $\overline{v\theta}$ was reproduced fairly well. Next, the validation was extended to the flow over a backward-facing step. In this case, the predicted results of wall shear stress coefficient (C_f) and Stanton number (St) were in good agreement with the relevant experiment. It was revealed that the present model prediction is in better agreement with the experiment than the case of $Pr_t = 1.0$. The assumption of $Pr_t = constant$ is inadmissible in the recirculating region.

Acknowledgements

This work was supported in part by the Korea Science and Engineering Foundation (KOSEF)

through the Advanced Fluids Engineering Research Center (AFERC), and in part by the National Research Laboratory of the Ministry of Science and Technology in Korea.

References

[1] T.S. Park, H.J. Sung, A new low-Reynolds-number model for predictions involving multiple surface, Fluid Dynamics Research 20 (1997) 97–113.
[2] T.S. Park, H.J. Sung, A nonlinear low-Reynolds-number k–ε model for turbulent separated and reattaching flows (I) flow field computations, Int. J. Heat and Fluid Flow 38 (1996) 2657–2666.
[3] G.B. Gatski, C.G. Speziale, On explicit algebraic stress models for complex turbulent flows, J. Fluid Mech 254 (1993) 59–78.
[4] F.S. Lien, P.A. Durbin, S. Parneix, Non-linear $\overline{v^2}$–f modelling with application to aerodynamic flows, in: Proc. 11th Symp. on Turbulent Shear Flows, 1997, pp. 6.19–6.24.
[5] C.G. Speziale, A consistency condition for non-linear algebraic Reynolds stress models in turbulence, Int. J. Non-linear Mechanics 33 (4) (1998) 579–584.
[6] S.B. Pope, Consistent modeling of scalars in turbulent flows, Phys. Fluid 26 (1983) 404–408.
[7] G.H. Rhee, H.J. Sung, A low-Reynolds-number, four-equation heat transfer model for turbulent separated and reattaching flows, Int. J. Heat and Fluid Flow 18 (1997) 38–44.
[8] J.C. Vogel, J.K. Eaton, Combined heat transfer and fluid dynamic measurements downstream of a backward-facing step, Trans. ASME J. Heat and Mass Transfer 107 (1985) 922–929.
[9] P.A. Durbin, D. Laurence, Nonlocal effects in single point closure, in: 3rd Advances in Turbulence Research Conference, 1996, pp. 109–120.
[10] R. Rubinstein, J.M. Barton, Nonlinear Reynolds stress models and the renormalization group, Phys. Fluid A 2 (1990) 1472–1476.
[11] A. Yoshizawa, Statistical analysis of the deviation of the Reynolds stress from its eddy viscosity representation, Phys. Fluids 27 (1984) 1377–1387.
[12] C.G. Speziale, S. Sarkar, T.B. Gatski, Modeling the pressure–strain correlation of turbulence: an invariant dynamical systems approach, J. Fluid Mech 227 (1991) 245–272.
[13] M.M. Gibson, B.E. Launder, Ground effects on pressure fluctuations in the atmospheric boundary layer, J. Fluid Mech 86 (1978) 491–511.
[14] M.M. Rogers, N.N. Mansor, W.C. Reynolds, An algebraic model for the turbulent flux of a passive scalar, J. Fluid Mech 203 (1989) 77–101.
[15] J. Kim, P. Moin, Transport of passive scalars in a turbulent channel flow, in: Proc. 6th Symp. on Turbulent Shear Flows, 1987, pp. 5.2.1–5.2.6.
[16] N. Kasagi, Y. Tomita, A. Kuroda, Direct numerical simulation of passive scalar field in a turbulent channel flow, Trans. ASME J. Heat and Mass Transfer 114 (1992) 598–606.
[17] Y. Nagano, H. Hattori, K. Abe, Modeling the turbulent heat and momentum transfer in flows under different thermal conditions, Fluid Dynamics Research 20 (1997) 127–142.
[18] R.M.C. So, T.P. Sommer, An explicit algebraic heat-flux model for the temperature field, Int. J. Heat and Mass Transfer 39 (3) (1996) 455–465.
[19] Y. Shabany, P.A. Durbin, Explicit algebraic scalar flux approximation, AIAA J 35 (6) (1997) 985–989.
[20] G.H. Rhee, H.J. Sung, A nonlinear low-Reynolds-number k–ε model for turbulent separated and reattaching flows. Part II: thermal field computations, Int. J. Heat and Mass Transfer 39 (1996) 3465–3474.
[21] K. Abe, T. Kondoh, Y. Nagano, A new turbulence model for predicting fluid flow and heat transfer in separating and reattaching flows—II. Thermal field calculations, Int. J. Heat and Mass Transfer 38 (1995) 1467–1481.
[22] B.E. Launder, B.I. Sharma, Application of the energy dissipation model of turbulence to the calculation of flow near a spinning disc, Lett. Heat and Mass Transfer 1 (1974) 131–138.
[23] D.M. Driver, H.L. Seegmiller, Features of a reattaching turbulent shear layer in divergent channel flow, AIAA J 23 (1985) 163–171.
[24] J.K. Eaton, J.P. Johnston, Turbulent flow reattachment: an experimental study of the flow and structure behind a backward-facing step, MD-39, Stanford University, 1980.